Hot carrier cooling by acoustic phonons in epitaxial graphene by ultrafast pump-probe spectroscopy

Dong Sun[1], Charles Divin[1], Claire Berger[2], Walt A. de Heer[2], Phillip N. First[2], and Theodore B. Norris[*, 1]

[1] Center for Ultrafast Optical Science, University of Michigan, 2200 Bonisteel Blvd., 48109 Ann Arbor, USA
[2] School of Physics, Georgia Institute of Technology, 30332 Atlanta, USA

* Corresponding author: e-mail tnorris@umich.edu, Phone: +001 734 764 9269, Fax: +001 734 763 4876

We report the application nondegenerate ultrafast mid-infrared spectroscopy to investigate the acoustic phonon cooling process in epitaxial graphene. We show that the power-dependent experimental results match theoretical predictions of the low temperature acoustic cooling process. The hot phonon effect in acoustic phonon cooling is observed experimentally, and a deformation potential of 30 eV can be determined from fitting the data.

1 Introduction Graphene grown epitaxially on SiC substrates is being actively researched as a highly promising platform for high speed carbon-based nanoelectronic and optoelectronic devices [1-3]. In high-speed devices, due to the presence of time-dependent high electric fields, carriers gain energy much faster than they are able to lose energy to the lattice, leading to a significantly elevated electron temperature T_e [4]. As the transport properties at high field are dominated by hot carriers, the understanding of cooling processes of hot carriers in multilayer epitaxial graphene (MEG) through the energy exchange between carriers in adjacent layers, the graphene lattice, and the heat dissipation to the SiC substrate, are crucial to high speed electronic device applications.

Ultrafast pump probe spectroscopy has been proven to be a powerful tool to time resolve the cooling of hot carriers in multilayer epitaxial graphene [5]. During the 100 fs pump pulse excitation, the hot electrons thermalize through sub-30 fs electron-electron scattering [6] and reach a quasi-equilibrium state with electron temperature above 1000 K. Since the electron heat capacity depends on the doping intensity and the pump beam is attenuated by each graphene layer, the initial electron temperature in the top layers of the sample is higher. However, hot electrons can efficiently transfer heat and reach equilibrium between the layers through a very fast interlayer thermal coupling during the first few picoseconds [7]. At the same time, the

hot electrons within each layer relax to about 250-300 K via coupling to graphene optical phonon and possibly SiC substrate optical phonons [7]. Once the carrier temperature has fallen below about 300 K, the cooling is mainly determined by acoustic phonon emission; this process has been recently theoretically investigated in by Bistritzer and MacDonald [8].

In this paper, we use pump-probe spectroscopy to quantify the carrier cooling and fit the results to the Bistritzer and MacDonald theory. We pump at 800 nm and probe at 1.88 μm probe to study the low temperature acoustic cooling process in multilayer epitaxial graphene. By fitting power dependent low temperature cooling behaviour with rate equation predicted by Bistritzer and MacDonald, we can determine the lattice deformation potential.

2 Experiment Epitaxial graphene samples used in this work are grown by thermal desorption of Si atom from SiC substrate [9]. For samples grown on C-terminated face of single-crystal 4H-SiC, the adjacent graphene layer is electronically decoupled or very weakly coupled to other layers due to the rotational stacking order [10]. The sample used in the pump power dependent measurements reported here (Fig. 1) has 21 layers with the most heavily doped layer having a Fermi level 348 meV above the Dirac point determined from previous ultrafast spectroscopy measurements [5]. The doping density and charge distribution

of C-face multilayer epitaxial graphene (MEG) samples are determined by assuming the same screening length as found in previous ultrafast spectroscopy measurements on similar samples having 63 layers [11]. Generally, the first few layers are heavily doped by charge transferred from the graphene-SiC interface [12]. The doping density of the subsequent graphene layers decreases, asymptotically approaching approximately 10^{10} cm^{-2} with charge screening length of 1 layer [11].
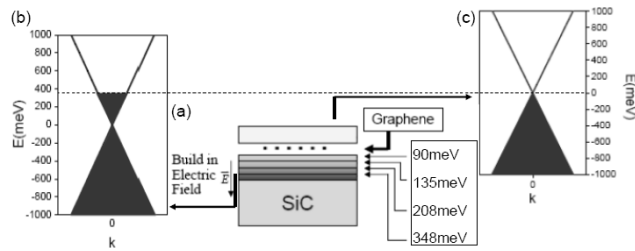

Figure 1 Sample structure and energy dispersion curve. (a) Sample structure of multilayer epitaxial graphene. The sample has a buffer layer on the SiC substrate. The subsequent layers are doped by charge transferred from the graphene-SiC interface. The Fermi levels of the first four layers are labeled. (b), (c) Energy dispersion curves of most heavily doped and undoped graphene layers. The Fermi level is labeled with a dashed line lying 348 meV above the Dirac point of the doped graphene layer and passing through the Dirac point of the undoped graphene layers.

For the infrared probe experiments, a 100-fs 250-kHz amplified Ti: sapphire laser at 800 nm pumps an infrared optical parametric amplifier (OPA) with signal wavelength tunable from 1.1 to 1.6 μm and idler wavelength tunable from 1.6-2.6 μm. The remnant 800 nm is compressed back below 100 fs and used as the pump. The OPA idler is tuned to 1.88 μm and used as probe. The pulse width of the OPA idler at the sample is estimated to be around 150 fs. The pump and probe are co-linearly polarized and focused to about 100-μm and 50-μm diameter spots respectively on the sample. The probe beam after the sample is detected by an InGaAs photo detector and lock-in amplifier referenced to the 4.2-kHz mechanically chopped pump. The sample temperature is cooled down to 10 K in a helium flow cryostat. The slight angle between the beams is sufficiently small to prevent temporal walk off across the relatively large probe spot.

3 Experimental result We excite the hot carriers with different initial electron temperatures by varying the 800 nm pump power, while probing (1.88 μm) just below the Fermi level of the first doped layer, but far above the Fermi level of all the other layers. We show below in our transfer matrix simulation that the selection of this specific probe wavelength guarantees that the DT signal at low temperature has the dominant contribution from the most heavily doped layer.
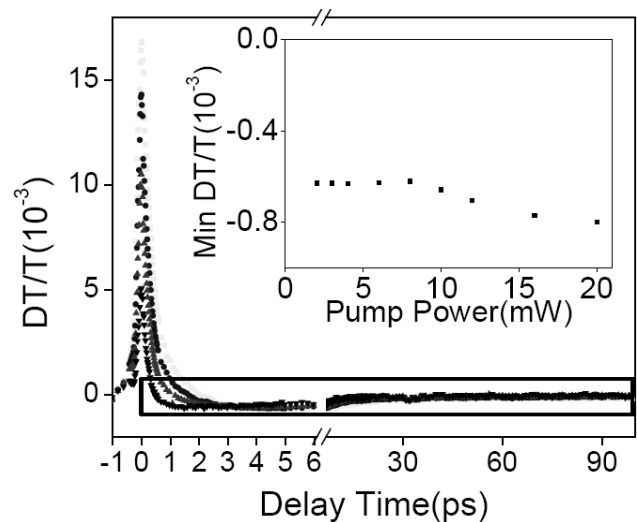

Figure 2 Pump power dependence. DT time scans with 800-nm pump and 1.8-μm probe at 10 K on a 21-layers MEG sample with 3 mW (down triangle), 6 mW (up triangle), 10 mW (dot) and 16 mW (grey rectangular) pump power respectively. The inset shows the minimum negative DT amplitude at several 800-nm pump powers.

The power-dependent data are shown in Fig. 2. After the initial thermalization and subsequent fast cooling during the first few picoseconds, the DT signal reaches a minimum negative point. Interestingly, as shown in the inset of Fig. 2, the minimum negative DT is almost a constant for relative low pump power excitations and only decreases slightly at high pump power. The DT relaxes to a flat negative value within 10s of ps delay depending on the pump power; this is a direct result of a higher lattice temperature at higher pump power. The cooling of the graphene lattice occurs finally through heat dissipation to the SiC substrate. This takes order longer than 100 ps which is beyond the largest experimental measured probe delay [7].

4 Transfer matrix simulation based on electron temperature dependent dynamics conductivity The differential transmission signal directly measured by the experiment can be related to the electron temperature of each graphene layer by a transfer matrix calculation. The transfer matrix of a graphene layer relates the incident and reflected probe fields via the dynamical conductivity σ of the layer [13]:

$$\begin{bmatrix} E_i^+ \\ E_i^- \end{bmatrix} = \begin{bmatrix} \dfrac{1}{2} + \dfrac{\eta_i}{2\eta_j} + \dfrac{\eta_i \sigma}{2} & \dfrac{1}{2} - \dfrac{\eta_i}{2\eta_j} + \dfrac{\eta_i \sigma}{2} \\ \dfrac{1}{2} - \dfrac{\eta_i}{2\eta_j} - \dfrac{\eta_i \sigma}{2} & \dfrac{1}{2} + \dfrac{\eta_i}{2\eta_j} - \dfrac{\eta_i \sigma}{2} \end{bmatrix} \begin{bmatrix} E_j^+ \\ E_j^- \end{bmatrix}$$

where $\eta_i = \sqrt{\mu_i / \varepsilon_i}$ is the dielectric impedance, and E_i^+, E_i^- are the incident and reflected fields, respectively, and E_j^+, E_j^- are the transmitted fields in the forward and backward directions. The conductivity is a function of electron temperature, so the transmission is a function of electron

temperature. We utilize a model for the conductivity including its dependence on electron temperature T_e and layer Fermi level µ [14]:

$$\sigma_{\alpha\beta}^{intra}(\omega) = \frac{-ie^2}{\hbar^2(\omega+i0)S} \sum_{\vec{k}l} \frac{\partial E_{\vec{k}l}}{\partial k_\alpha} \frac{\partial f(E_{\vec{k}l})}{\partial E_{\vec{k}l}} \frac{\partial E_{\vec{k}l}}{\partial k_\beta}$$

$$\sigma_{\alpha\beta}^{inter}(\omega) = \frac{ie^2\hbar}{S} \sum_{\vec{k},l\neq l'} \frac{f(E_{\vec{k}l'})-f(E_{\vec{k}l})}{E_{\vec{k}l'}-E_{\vec{k}l}-\hbar(\omega+i0)} \frac{1}{E_{\vec{k}l'}-E_{\vec{k}l}}$$

$$\cdot < \vec{k}l \mid \hat{v}_\alpha \mid \vec{k}l' >< \vec{k}l' \mid \hat{v}_\beta \mid \vec{k}l >$$

Here $E_{\mathbf{k}l} = (-1)^l \hbar V k$ is the eigenenergy spectrum for electron (l=1) and hole bands (l=2), and the corresponding wave functions are $\mid \mathbf{k}l\rangle$, $\alpha=(x,y)$, σ_α are Pauli matrixes, $\mathbf{k}=(k_x,k_y)$ and $k=\sqrt{k_x^2+k_y^2}$ is the wave vector, $f(E_{\mathbf{k}l})$ is the Fermi distribution function which is function of T_e and µ, $\hat{v}_\alpha = V\sigma_\alpha$ is the velocity operator, and S is the sample area.
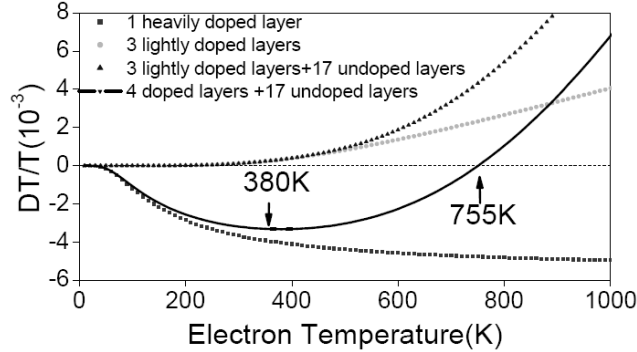

Figure 3 Transfer matrix simulation of the DT/T signal of MEG with different graphene layers combination at different electron temperatures.

The product of all transfer matrices, including that of the substrate, gives the optical response of the MEG sample. In the simulation we include four highly doped layers with charge densities corresponding to those measured in the experiment [11] and we further assume all graphene layers have the same electron temperature following the first few picoseconds initial cooling; this is a reasonable assumption considering the strong interlayer thermal coupling observed in a separate degenerate pump probe experiment [7]. A simulation of the DT signal at 1.88-µm probe wavelength as a function of electron temperature is shown in Fig. 3. We see that the DT response is dominated by the contribution of the first doped layer at low electron temperatures (below 300 K), so the DT tails unambiguously measure the relaxation of the hot carriers in the first doped layer when the electron temperature is below 300 K. This is not surprising since the probe photon energy is very close to the Fermi level of the first doped layer and far above the Fermi level of all other layers.

The simulation results including all layers in the sample show DT zero crossings around 750 K and a minimum negative DT round 380 K. Therefore when the electron

temperature relaxes to 380 K, the DT reaches the same negative DT amplitude regardless of the initial electron temperature at different pump excitations; this matches the experimental observation shown in the inset of Fig. 2. Thus the minimum negative DT is a clear experimental indicator of 380 K electron temperature.

5 Electron and lattice heat capacity in graphene
The electron heat capacity of the doped layer and undoped layer at relatively low electron temperature can be obtained from a simple statistical mechanical calculation. For undoped layers, the electron heat capacity has T_e^2 dependence:

$$C_e(T_e) = \frac{\partial E}{\partial T_e} = \frac{18\zeta_3}{\pi} k_B (\frac{k_B T_e}{\hbar v_F})^2$$

where T_e is the electron temperature, v_F is the Fermi velocity, k_B is the Boltzmann constant and $\zeta_3 = \int_0^\infty dx \frac{x^2}{e^x+1}$ is the Riemann zeta function, so for the undoped layers:
$$C_e^{undoped}(T_e) = 8.136588*10^{-13} T_e^2 (J/m^2 K)$$
For doped layers, the electron heat capacity has T_e dependence:

$$C_e(T_e) = \frac{1}{A} \frac{\partial U}{\partial T} = \frac{2\pi}{3} \frac{E_F^0}{\hbar^2 v_F^2} k_B^2 T_e,$$

where E_F is the Fermi level of the doped layer, for the heavily doped layer with Fermi level of 350 meV, $C_e^{doped}(T_e) = 2*10^{-9} T_e (J/m^2 K)$. At low temperature the lattice heat capacity is dominated by the acoustic phonons, in our simulation, we use a simple linear temperature dependent lattice heat capacity: fit from Mounet and Marzari's first principle calculation [15]:

$$C_l(T_l) = 1.3*10^{-6} T_l (J/m^2 K)$$

6 Fitting of low temperature acoustic phonon cooling Carrier cooling through acoustic phonon emission has been treated theoretically by R. Bistritzer and D. MacDonald [8] for both lightly- and heavily-doped graphene layers. In the neutral regime, the electron temperature is described by $\partial_t T_e = -\gamma T_e^2 (T_e - T_l)$, where T_e and T_1 are electron and lattice temperature respectively, $\gamma = 1.18*10^3 D^2 (meV^2 s)^{-1}$ and D is the deformation potential measured in eV. This equation applies to the large number of undoped layers in our multilayer epitaxial graphene sample at low carrier temperature. In contrast, the electron temperature in the heavily doped bottom layers follows $\partial_t T_e = -\gamma_d (T_e - T_l)/T_e$, where $\gamma_d = 0.133 D^2 n^{3/2} meV/ns$ with n being measured in units of 10^{12} cm^{-2}. This predicts an acoustic phonon cooling time on the order of 10 ps in the heavily doped layer which matches the measurements shown in Fig. 2.

Invited

Article

Since the heat capacity of the undoped layer is at least an order of magnitude smaller than that of the heavily doped layer at electron temperatures below 380 K, the effect of the interlayer thermal coupling on the cooling of the highly doped layer can be safely ignored in the simulation. The slow ns thermal coupling to the SiC substrate during the 10-40 ps acoustic cooling process was ignored in the simulation, and a constant lattice temperature was used in this low electron temperature cooling simulation due to the 3 orders larger lattice heat capacity compared to the electron heat capacity (the lattice temperature was estimated by assuming 2.3% of the pump energy is deposited to the electron gas in each graphene layer and then is transferred to the lattice). The ratio of energy loss via optical phonons to the energy loss vai the acoustic phonons for undoped and heavily doped layers at different carrier temperatures has been calculated by Bistritzer and MacDonald [8]. For the heavily doped layer, the optical phonon cooling shuts down completely at 250 K from their simulation, and at an electron temperature of 380 K, this ratio is below 20%. In our simulations, the energy relaxation through optical phonon between 250 K and 380 K is ignored; this will make the simulation results slower than the experiment in this temperature range. Another important process that is not included in our simulation is the decay of the hot optical phonon to the acoustic phonon mode in the first few ps, the life time of optical phonon in graphene has been measured to be 2.5 ps [16]. This contribution accounts for the relatively slower simulated cooling at high electron temperature before the decay of optical phonons and relative faster simulated cooling when all optical phonons decays to acoustic phonons.
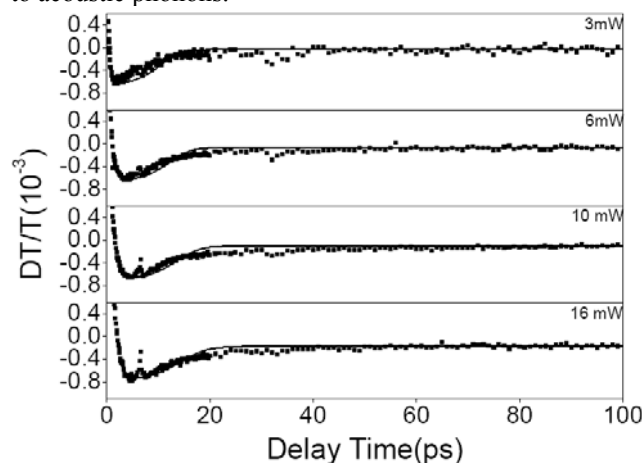

Figure 4 Acoustic phonon cooling fitting. The measured DT signal (dots) at low temperature is plotted along with the theoretical acoustic phonon cooling model (solid).

Figure 4 shows a fit of the low energy acoustic phonon cooling process in the heavily doped layers starting from 380 K which can be identified from the minimum negative DT in the experimental differential transmission curve. Besides the secondary peaks at ~6 ps and ~30 ps due to

back reflection of pump pulse in SiC substrate and CaF_2 crystat windows, the experimental result is well fit with a deformation potential of ~30 eV which is within the 20 and 50 eV range bounded by transport measurements [17].

7 Conclusion We have applied pump power dependent nondegenerate ultrafast infrared spectroscopy to investigate the acoustic phonon cooling process in the most heavily doped layer in multilayer epitaxial graphene. We show that the experimental differential transmission recovery can be well fit by the theoretically predicted low temperature acoustic cooling process. We also determine the deformation potential to be 30 eV from our experiment.

References

[1] Y. Zhang et al., Nature **459**, 820 (2009).
[2] W. A. de Heer et al., Solid State Commun. **143**, 92 (2007).
[3] C. Berger et al., J. Phys. Chem. B **108**, 19912 (2004).
[4] O. G. Balev, F. T. Vasko, and V. Ryzhii, Phys. Rev. B **79**, 165432 (2009).
[5] D. Sun et al., Phys. Rev. Lett. **101**, 157402 (2008).
[6] M. Breusing, C. Ropers, and T. Elsaesser, Phys. Rev. Lett. **102**, 086809 (2009).
[7] D. Sun et al., to be submitted 2010.
[8] R. Bistritzer and A. H. MacDonald, Phys. Rev. Lett. **102**, 206410 (2009).
[9] C. Berger et al., Science **312**, 1191 (2006).
[10] J. Hass et al., Phys. Rev. Lett. **100**, 125504 (2008).
[11] D. Sun et al., Phys. Rev. Lett. **104**, 136802 (2010).
[12] F. Varchon et al., Phys. Rev. Lett. **99**, 126805 (2007).
[13] M. Born, and E. Wolf, Principles of Optics (Cambridge University Press, 1999).
[14] S. A. Mikhailov and K. Ziegler, Phys. Rev. Lett. **99**, 016803 (2007).
[15] N. Mounet and N. Marzari, Phys. Rev. B **71**, 205214 (2005).
[16] H. Wang et al., Appl. Phys. Lett. **96**, 081917.
[17] K. I. Bolotin et al., Phys. Rev. Lett. **101**, 096802 (2008).